

# Prediction of amyloidogenicity based on the n-gram analysis

Michał Burdukiewicz<sup>1</sup>, Piotr Sobczyk<sup>2</sup>, Stefan Rödiger<sup>3</sup>, Anna Duda-Madej<sup>4</sup>, Paweł Mackiewicz<sup>1</sup> and Małgorzata Kotulska<sup>5</sup> \*

<sup>1</sup>University of Wrocław, Department of Genomics, <sup>2</sup>Wrocław University of Science and Technology, Department of Mathematics <sup>3</sup>Brandenburg University of Technology Cottbus-Senftenberg, Institute of Biotechnology <sup>4</sup>Wrocław Medical University, Department of Microbiology and <sup>5</sup>Wrocław University of Science and Technology, Department of Biomedical Engineering, Faculty of Fundamental Problems of Technology

Received on XXXXX; revised on XXXXX; accepted on XXXXX

## ABSTRACT

Text. Text. Text. Text. Text. Text. Text. Text. Text. Text.  
Text. Text. Text. Text. Text. Text. Text. Text. Text. Text.  
Text. Text. Text. Text. Text. Text. Text. Text. Text. Text.  
Text. Text. Text. Text. Text. Text. Text. Text. Text. Text.  
Text. Text. Text. Text. Text. Text. Text. Text. Text. Text.  
Text. Text. Text. Text. Text.

## INTRODUCTION

Amyloid aggregates have been observed in tissues of people suffering from various diseases, such as: Alzheimer's, Parkinson's, amyotrophic lateral sclerosis and Huntington's, as well as many other conditions. These aggregates were also detected in diseases other than neurological, for example in diabetes of type 2 or certain types of a cataract. Cells in tissues with amyloid fibrils exhibit very high mortality. However, the mechanisms of the cytotoxicity have not been discovered. The aggregates are very stable and their dissolution is very difficult. Amyloids are resistant to activity of proteolytic enzymes and chemical compounds due to the specific and highly ordered structure of their steric zipper. However, some strategies to prevent amyloid formation have been proposed (1).

The aggregation occurs when a cell environment fosters the partial unfolding of protein chains or their fragmentation in such a way that the parts prone to joining with other protein fragments become exposed. For the majority of proteins, considerable conformational rearrangement must have occurred to initiate the aggregation process. Such changes cannot take place in the typical tightly packed native protein conformation due to the constraints of the tertiary structure. Thus, the formation of a non-native partially unfolded conformation is required to start the aggregation presumably by enabling specific intermolecular interactions including electrostatic attraction, hydrogen bonding and hydrophobic contacts. This partial unfolding can be influenced by various factors, such as high concentration of proteins, high temperature, low pH, binding metals, or exposition to UV light.

Initially, the resulting molecules form clusters consisting of a few elements, which are called oligomers. Next, they grow into larger aggregates. The aggregation of proteins or their fragments may lead to amorphous (unstructured) clusters or amyloid (highly ordered) unbranched fibrils. Independently of the protein sequence and its original structure, aggregates always display a common cross- $\beta$  structure. The distinctive structure of the steric zipper enables the selective detection of amyloids from amorphous aggregates using either a variety of microscopic techniques or fluorescence of probes with which they form compounds.

Currently, it is believed that short peptide sequences of amyloidogenic properties, called hot spots, are responsible for the aggregation of amyloid proteins. Previous studies have suggested that amyloidogenic fragments may have regular characteristics, not only with regard to averaged physicochemical properties of their amino acids, but also the order of amino acids in the sequence. It is important to distinguish between amyloidogenic and amyloidic regions because only the former initiate the process of the aggregation and the latter consist of all regions involved in the creation of the final aggregate. Several computational approaches were proposed to model and predict both kinds of regions. Physics- and chemistry-based models used in FoldAmyloid (2) utilize the density of the protein contact sites. Other methods perform threading a peptide on an amyloid fiber backbone, followed by determination of its energy and stability (3, 4, 5). Statistical approaches include production of frequency profiles, such as the WALTZ method (6) and machine learning methods, which have been developed by our team (7, 8). AGGRESCAN3D has been proposed to estimate more accurately aggregation propensity by performing 3D structure based analysis (9).

The majority of methods described above uses theoretical knowledge to specify decision rules determining the presence of the hot spot. The aim of our study is opposite, because out of thousands of created hot spot models, we choose the most appropriate.

In bioinformatics, n-grams (k-mers) are continuous or discontinuous sequences of  $n$  elements. Employed as a feature extraction method, n-grams are widely used in analysis of

\*To whom correspondence should be addressed. Email: malgorzata.kotulska@pwr.edu.pl

© 2015 The Author(s)

This is an Open Access article distributed under the terms of the Creative Commons Attribution Non-Commercial License (<http://creativecommons.org/licenses/by-nc/2.0/uk/>) which permits unrestricted non-commercial use, distribution, and reproduction in any medium, provided the original work is properly cited.

biological sequences. Our choice of n-grams was driven by their highly interpretable nature. This is a valuable feature because we are interested in identification of motifs that are most relevant to amyloidogenic properties of peptides. The most discriminating n-grams were extracted using a novel feature selection algorithm called Quick Permutation Test (QuiPT).

Several studies highlighted that three-dimensional protein structure depends not on the exact sequence of amino acids but on their general physicochemical properties. Hence, a reduction of 20 amino acid alphabet by an appropriate encoding amino acids into more general symbols can still retain the information about the protein folding (10). Since amyloid aggregates, especially their hot spots regions, have very specific spatial organization, we investigated if these regions can be also described by a shorter amino acid alphabet (encoding). Instead of relying on the general similarities of amino acids, we created multiple encodings based on the combinations of various physicochemical properties that might be associated with amyloidogenicity.

To discover amino acid patterns specific for amyloidogenic peptides we based our analysis on n-grams, continuous or discontinuous sequences of length  $n$ . Extraction of n-grams allows detection of more elaborated motifs, but creates very large features spaces. Henceforth, we used Quick Permutation Test (QuiPT) to select only informative n-grams drawn from peptides encoded with the reduced amino acid alphabet.

We used selected n-grams to train a predictor based on random forest (11) discriminating between amyloidogenic and non-amyloidogenic peptides. We trained several iterations of a classifier using peptides with different length to identify the optimal number of residues which include the information about the presence or absence of hot spots. In the cross-validation setup we found the encoding associated with the best-performing classifier and its set of informative n-grams.

## METHODS

### Data set

The data used in the study was extracted from AmyLoad data base (12). We obtained 418 amyloidogenic peptides and 1039 non-amyloidogenic peptides.

Sequences shorter than six and longer than 25 amino acid residues (i.e., 8 and 27 sequences, respectively) were removed from the set. The former were too short to be processed in the devised n-gram analysis framework and the latter were too diversified and rare, hampering the proper analysis.

The final data set contained in total 1430 peptides: 397 amyloidogenic and 1033 non-amyloidogenic sequences.

### Encodings of amino acids

The amyloidogenicity of a given peptide may not depend on the exact sequence of amino acids but on its more general properties. To verify this hypothesis, we handpicked 20 measures from AAIndex database (13) describing features important in the amyloidogenicity, such as: size of residues, hydrophobicity, solvent surface area, frequency in  $\beta$ -sheets and contactivity. We selected them among properties that were introduced after 1980 when, thanks to the technological advancements, the measurements were more accurate than the

older ones. The set of selected physicochemical properties was enriched by six measures representing amino acid contact site propensities (14) giving in total 26 features.

Since highly correlated measures would create very similar amino acid encodings, we further reduced the number of properties to 17 by selecting measures with the absolute value of Pearson's correlation coefficient smaller than 0.95 (Tab. 1).

Based on that, we created 524,284 amino acid encodings with different level of amino acid alphabet reduction from three to six amino acid groups using Ward's clusterization (15), which was performed on all combinations of the normalized values of physicochemical properties from 1 to 17.

The majority of encodings had at least one duplicate. In such case, only a single representative was included in the cross-validation. After filtering the duplicates, we obtained 18,535 unique encodings.

**Table 1.** Selected 17 physicochemical properties used to create amino acid encodings.

Category	Property
Contactivity	Average flexibility indices (16)
Contactivity	14 Å contact number (17)
Contactivity	Accessible surface area (18)
Contactivity	Buriability (19)
Contactivity	Values of $W_c$ in proteins from class $\beta$ , cutoff 12 Å, separation 5 (14)
Contactivity	Values of $W_c$ in proteins from class $\beta$ , cutoff 12 Å, separation 15 (14)
$\beta$ -frequency	Average relative probability of inner beta-sheet (20)
$\beta$ -frequency	Relative frequency in $\beta$ -sheet (21)
$\beta$ -frequency	Thermodynamic $\beta$ -sheet propensity (22)
Hydrophobicity	Hydrophobicity index (23)
Hydrophobicity	Optimal matching hydrophobicity (24)
Hydrophobicity	Hydrophobicity-related index (25)
Hydrophobicity	Scaled side chain hydrophobicity values (26)
Polarity	Polarizability parameter (27)
Polarity	Mean polarity (18)
Size	Average volumes of residues (28)
Stability	Side-chain contribution to protein stability (kJ/mol) (29)

### Training sets

In the initial phase, we extracted overlapping hexamers from each peptide sequence. Each hexamer was tagged with the same etiquette (amyloid/nonamyloid) as the source peptide. (Fig. 1 A and B).

Assuming that only a short part of the sequence in longer amyloids is responsible for amyloidogenicity, our method might result in many false positives in the training data set and in consequence yield inaccurate predictions as it was evaluated elsewhere (30). To diminish this problem and facilitate the extraction of hot spots, we restricted the maximum length of peptides in training data set to fifteen amino acids.

To further study the problem of the amyloidogenicity signal length, we created three learning sets with the sequences of different lengths (Tab. 2). The smallest data set contained only the sequences of length 6. Assuming that the minimum length of the amyloidogenicity signal is the six residues, we can

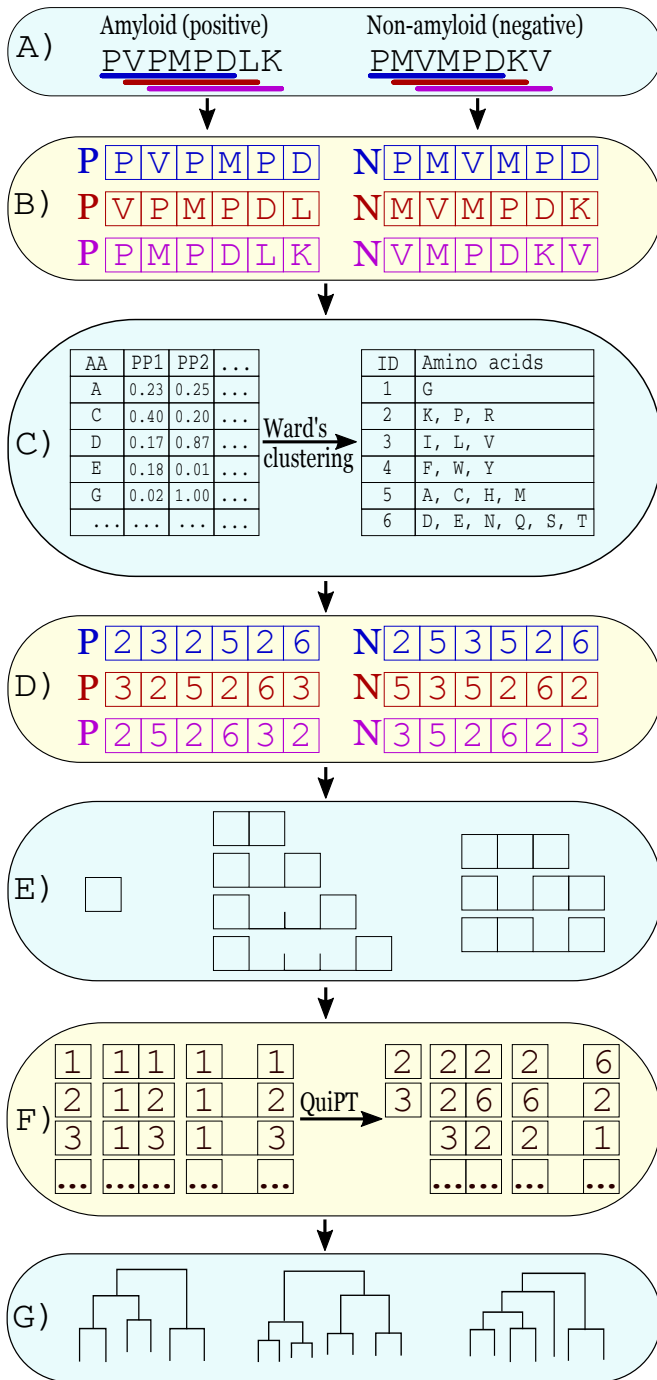


**Figure 1.** The scheme of n-gram extraction from studied peptide sequences. A) Source data: peptides with known amyloidogenicity status and indicated overlapping hexamers. B) Extraction of the overlapping hexamers and ascription to them of the amyloidogenicity status taken from their source peptide (P-positive, N - negative). C) Clusterization of amino acids into an encoding using a combination of various physicochemical properties (PP). D) Reduction of the amino acid alphabet in hexamers. E) Extraction of n-grams. From each hexamer, we extracted continuous n-grams with the length  $n = 1, 2$  or  $3$ . In addition, we selected gapped 2-grams with a gap of the length from 1 to 3 residues and gapped 3-grams with a single gap between the first and the second or the second and the third element of the n-gram. F) Selection of informative n-grams with Quick Permutation Test (QuiPT). G) Training of a random forest classifier using n-grams selected in the previous step.

**Table 2.** Characteristics of training and test data sets used in the analysis.

Set	Sequence length	Status	Sequences	Hexamers
Training	6	Non-amyloid	841	841
		Amyloid	247	247
	[6,10]	Non-amyloid	964	1412
		Amyloid	312	475
	[6,15]	Non-amyloid	992	1653
		Amyloid	342	720
Test	6	Non-amyloid	841	841
		Amyloid	247	247
	[6,10]	Non-amyloid	123	571
		Amyloid	65	228
	[11,15]	Non-amyloid	28	241
		Amyloid	30	245
	[16,25]	Non-amyloid	41	571
		Amyloid	55	778

expect no false positive hexamers. Moreover, we created two training sets with the progressively more liberal limit of the maximum sequence length (6-10 residues and 6-15 residues).

From each hexamer we extracted n-grams with the length of 1, 2 and 3. In the case of 2- and 3-grams, we separately analyzed continuous and gapped n-grams. For 2-grams, we considered n-grams with the gap of the length from 1 to 3, whereas the 3-grams could contain a single gap between the first and the second or the second and the third position (see Fig. 1). The total number of n-grams depends on the the length of the encoding and is equal to 120, 260, 480 and 798 for encodings of length 3, 4, 5 and 6 respectively.

Furthermore, we repeated the procedure described above on two standard encodings derived from the literature to check if the process of amyloidogenicity does require nonstandard groupings of amino acids. We also added the full (unreduced) amino acid alphabet with 25,620 n-grams to assess the advantages of the amino acid encoding.

### Quick Permutation Test (QuiPT)

All n-grams extracted from the hexamers in the training data set were filtered using the Quick Permutation Test with the information gain (mutual information) as the criterion of the importance of a specific n-gram. Only n-grams with the p-value smaller than 0.05 were assumed to be informative.

The permutation tests are commonly used for filtering important n-grams. However, they are computationally expensive and as a result, they often become one of the most limiting factors for these kinds of analyses. The Quick Permutation Test effectively filters n-gram features without performing a huge number of permutations. Let us consider a contingency table for a target  $y$  and a feature  $x$ . For example, the entry  $n_{1,0}$  is the number of cases when the target is 1 and the feature is 0.

target / feature	1	0	total
1	$n_{1,1}$	$n_{1,0}$	$n_{1,\cdot}$
0	$n_{0,1}$	$n_{0,0}$	$n_{0,\cdot}$
total	$n_{\cdot,1}$	$n_{\cdot,0}$	$n$

Under the hypothesis that  $x$  and  $y$  are independent, the probability of observing such a contingency table is given by the multinomial distribution. The idea of permutation test is to reshuffle labels of features and targets but keeping the fixed total number of positives for features and targets. When we impose this constraint on the multinomial distribution, then the probability of occurrence for a given contingency table depends only on one entry, i.e.,  $n_{1,1}$ , which is fairly easy to compute. After computing Information Gain (IG) for each possible value of  $n_{1,1} \in [0, \min(n_{1,\cdot}; n_{\cdot,1})]$ , we get the distribution of Information Gain under hypothesis that the target and feature are independent. We reject null hypothesis, when IG for the tested feature is above the required quantile from the IG distribution.

The analytic formula for the distribution enables to perform the permutation test much quicker. Furthermore, we get exact quantiles even for extreme tails of the distribution, which is not guaranteed by the random permutations. For example, for the test with  $\alpha = 10^{-8}$ , which can often occur in the corrections for multiple testing, the standard deviation of quantile estimate in permutation test,  $\frac{p(1-p)}{m}$ , is roughly equal to  $\alpha$  itself even for a huge number of permutations like  $m = 10^8$ .

In the context of  $n$ -gram data, we can further speed up our algorithm. Note that test statistics depends only on  $n_{\cdot,1}$ , i.e., the number of positive cases in the feature when the target  $y$  is common for testing all  $n$ -gram features. Although we test millions of features, there are only a few distributions that we need to compute because the usually number of positives in  $n$ -gram feature is small. We take advantage of this fact and we compute quantiles only for the handful of distributions. Therefore complexity of our algorithm is roughly equal  $O(n \cdot p)$ .

Lastly, let us point out that QuiPT is very similar to Fisher's exact test. From the derivation provided in, e.g. (31), it becomes obvious that QuiPT is a heuristics for an unsolved problem of a two-tailed Fisher's exact test. In this heuristics, the extremity of a contingency table is defined by its Information Gain.

### Random forest classifier

During the learning stage, random forest classifier was trained on the  $n$ -grams drawn from overlapping hexamers considering only  $n$ -grams selected by QuiPT. We grown forest with default parameters: 500 trees and the number of variables to possibly split at in each node equal to the (rounded down) square root of the total number of variables. The employed random forest implementation is using ranger **R** package (32).

The predictor separately considered all hexamers coming from a single peptide. If at least one hexamer extracted from a peptide was assessed as amyloidogenic, the whole sequence was denoted as amyloid. Otherwise, the peptide was classified as non-amyloid. The results were next compared with the known etiquette of the peptides to compute the performance measures.

### Cross-validation and selection of the best-performing encoding

The ability to correctly predict amyloidogenicity of peptides was assessed during the five-fold cross-validation. The

peptides were assigned randomly to subsamples. Since this approach may result in the uneven number of hexamers in the subsamples (longer peptides yields more hexamers than shorter ones), we repeated the cross-validation fifteen times for each classifier to obtain more precise estimates of performance measures.

To evaluate if our classifiers are able to use decision rules extracted from sequences of given length to correctly classify longer or shorter sequences, we cross-validation.

To choose the most adequate amino acid encoding, we ranked the values of Area under Curve (AUC) for the particular classifiers (with rank 1 for the best AUC, rank 2 for the second best AUC and so on) and various ranges of sequence length in the testing data set. The encoding with the lowest sum of ranks from all sequence length categories was selected as the best one. For this encoding, we choose the range of peptides length in the training set that provided the best AUC in the cross-validation.

### Encoding distance

To compare obtained encodings, we introduced the encoding distance, which is a measure defining the similarity between two encodings. It has zero value for identical encodings and grows with the differences between the encodings. This parameter enabled us to select the reduced alphabets that were very similar to the best one and verify if they also show the good prediction performance.

We define the encoding distance as the minimum number of amino acids that have to be moved between subgroups of the encoding  $a$  to make it identical to the encoding  $b$  (the order of subgroups in encodings and the order of amino acids in groups are not important). This measure was further scaled by a factor reflecting how much moving amino acids between groups altered the mean value of physicochemical properties in the group.

To compute the scale factor  $s$  for the encoding distance between the encoding  $a$  with  $n$  subgroups (enumerated with  $i$ ) and the encoding  $b$  with  $m$  subgroups (enumerated with  $j$ ), we first calculated  $p_i$  and  $q_j$ , i.e. the mean values of physicochemical properties of all amino acids for each subgroup. The factor  $s$  between encodings  $a$  and  $b$  is equal to:

$$s_{ab} = \sum_{i=1}^n \left( \min_{j=1, \dots, m} \sum_{l=1}^L \sqrt{(p_{i,l} - q_{j,l})^2} \right)$$

where  $L$  is the number of considered physicochemical properties. Hence, the normalizing factor may be interpreted as the minimum change of the mean physicochemical properties between groups.

### Benchmark of AmyloGram

The best-performing encoding chosen during the cross-validation was later used to train AmyloGram,  $n$ -gram based predictor of peptide amyloidogenicity.

To compare the performance of AmyloGram and other predictors of amyloids we used external data set *pep424* (33). Since some peptides were common for both *pep424* and AmyLoad, we removed them from the training data set.

After the purification, the learning data set for purposes of benchmark consisted of 269 positive sequences and 746 negative sequences longer than five and shorter than fifteen residues.

We removed peptides shorter than five amino acids from the *pep424* data set as they are shorter than minimum length assumed in our model of amyloidogenicity. This change should not have affected the comparison as only five sequences were eliminated (around 1% of the original data set). Besides the classifier based on the reduced amino acid alphabet, we also benchmarked three predictors based on the full 20-amino acid alphabet learned on *n*-grams extracted from sequences with different length ranges to separately assess the benefit of using only the *n*-gram analysis without the reduction of amino acid alphabet.

## RESULTS AND DISCUSSION

### Performance of the best encoding

The selected encoding performed better than other reduced alphabets considering all ranges of sequence lengths in the training and testing data set. It had the AUC always in the fourth quartile of other encodings (Fig. 2). The best encoding reached the highest values of AUC (=...) in the recognition of the shortest sequences (with 6 residues) when the training set also consisted of the sequences with the same length. It may result most probably from the homogeneity of the short peptides. Nevertheless, the results were quite comparable even if the training set contained longer sequences. By average, the majority of encodings behaved like the selected encoding and also received higher AUC for the shorter tested sequences than for the longer ones. For the best-performing encoding, the most problematic was the correct prediction of the amyloidogenicity in the longest peptide from 16 to 25 residues, when the algorithm was learned also on longer peptides (6-10 and 6-15 data sets).

The weakest performance measured by AUC for sequences longer than 15 amino acids results from difficulties in extraction of the important discriminating features related with more complex organization of longer amyloidogenic peptides. In such peptides, only a very specific region of residues might be responsible for the creation of harmful aggregates. In this case, when overlapping hexamers are extracted, only part of them may carry the true signal of amyloidogenicity but all of them are marked as amyloids. However, despite this problem, the overall prediction of classifiers learned on the long sequences was still adequate, with the median values of AUC higher than 0.7 for every testing set.

In addition to the high AUC, the best encoding had also very good sensitivity and specificity regardless of the length of sequences in training and tested set (Fig. 3). The classifiers trained on the peptides with the length 6 tended to have the best specificity, whereas predictors learned on the long sequences had the best sensitivity. Although the classifiers trained on the six-residue-long sequences had generally the better AUC, their training on the sequences from six to ten residues seems to yield the most balanced classifiers with the optimal sensitivity and specificity.

We also evaluated classifiers based on the full (i.e., unreduced) amino acid alphabet. In most cases, they were

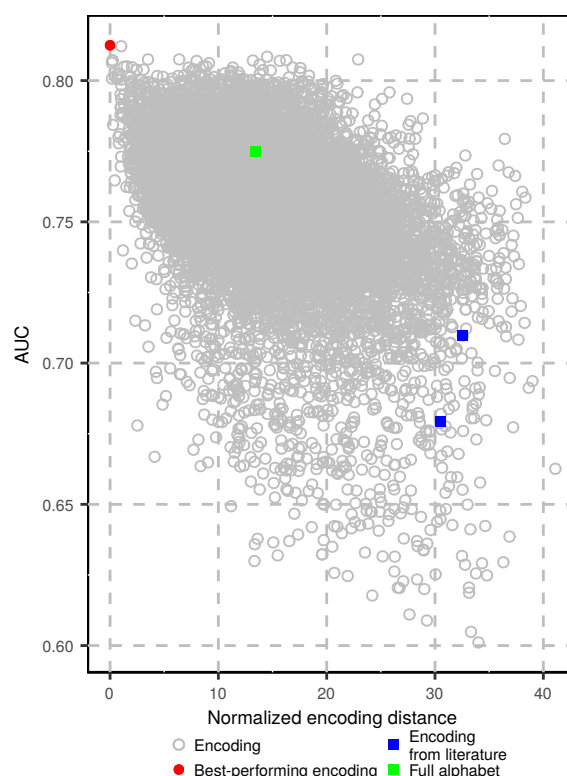


**Figure 4.** The encoding distance and AUC of the reduced alphabets studied in the cross-validation. Classifiers with the smallest encoding distance to the best classifier have the highest AUC.

also placed in the fourth quartile of AUC value (Fig. 2). Nevertheless, they never predicted amyloidogenicity better than the best classifier based on the reduced alphabet. It indicates that despite a lot of information present in the full alphabet, the encoding allows better generalization of the prediction rules and in the consequence a better performance.

Similarly to the best-performing encoding, the sensitivity of classifiers based on the full amino acid alphabet decreased with the length of sequences in the training data set (Fig. 3). Furthermore, these classifiers always seemed to have one of the worst sensitivities among all analyzed predictors, especially when tested on the longer amyloids. It means that using the full amino acid alphabet it was easier to point the non-amyloidogenic sequences instead of amyloids.

The standard encodings found in the literature perform significantly worse than other analyzed encodings in all categories. It indicates that the descriptive divisions of amino acids do not create groups suitable for the recognition of amyloids. This observation is well-supported by the specificity-sensitivity plot (Fig. 3), where classifiers trained with this encodings of amino acids groups belong to the worst performers.

### The best-performing encoding and important *n*-grams

In total, eleven combinations of physicochemical properties created the best performing encoding. Only four features appeared in all combinations: hydrophobicity index (23), average flexibility indices (16), polarizability parameter (27) and thermodynamic  $\beta$ -sheet propensity (22).

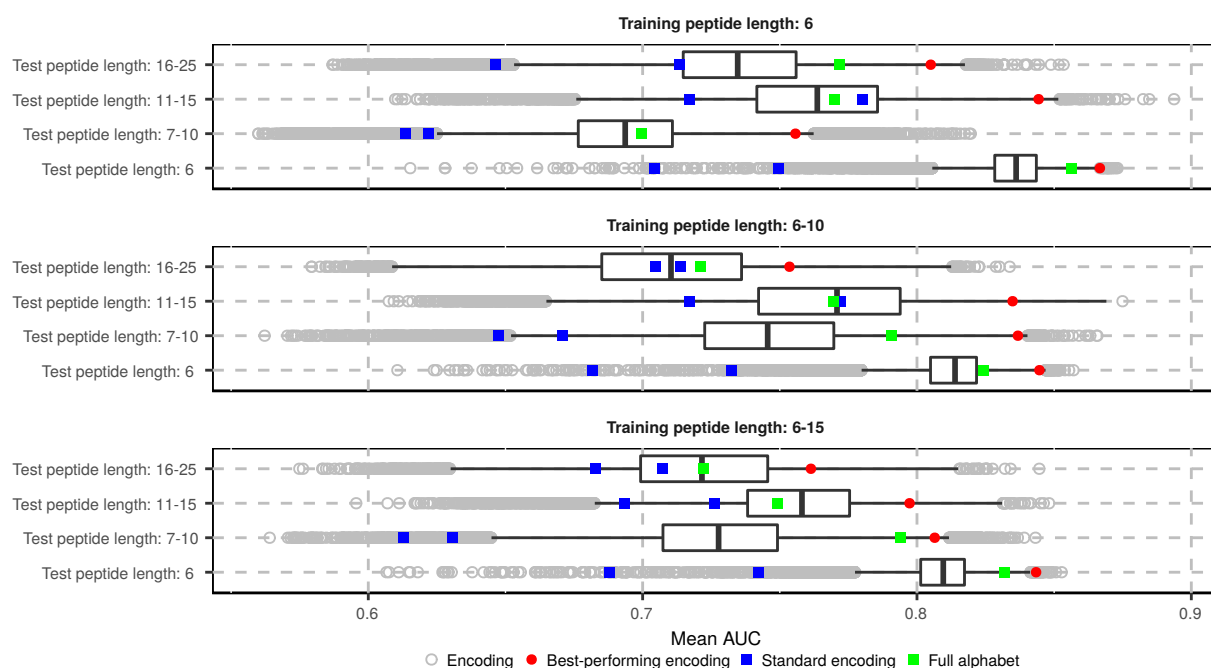


**Figure 2.** Distribution of mean AUC values of classifiers with various encodings for every possible combination of training and testing data set including different lengths of sequences. The left and right hinges of boxes correspond to the 0.25 and 0.75 quartiles. The bar inside the box represents the median. The gray circles correspond to the encodings with the AUC outside the 0.95 confidence interval. The best-performing encoding was best by average for various ranges of sequence length in the testing data set.

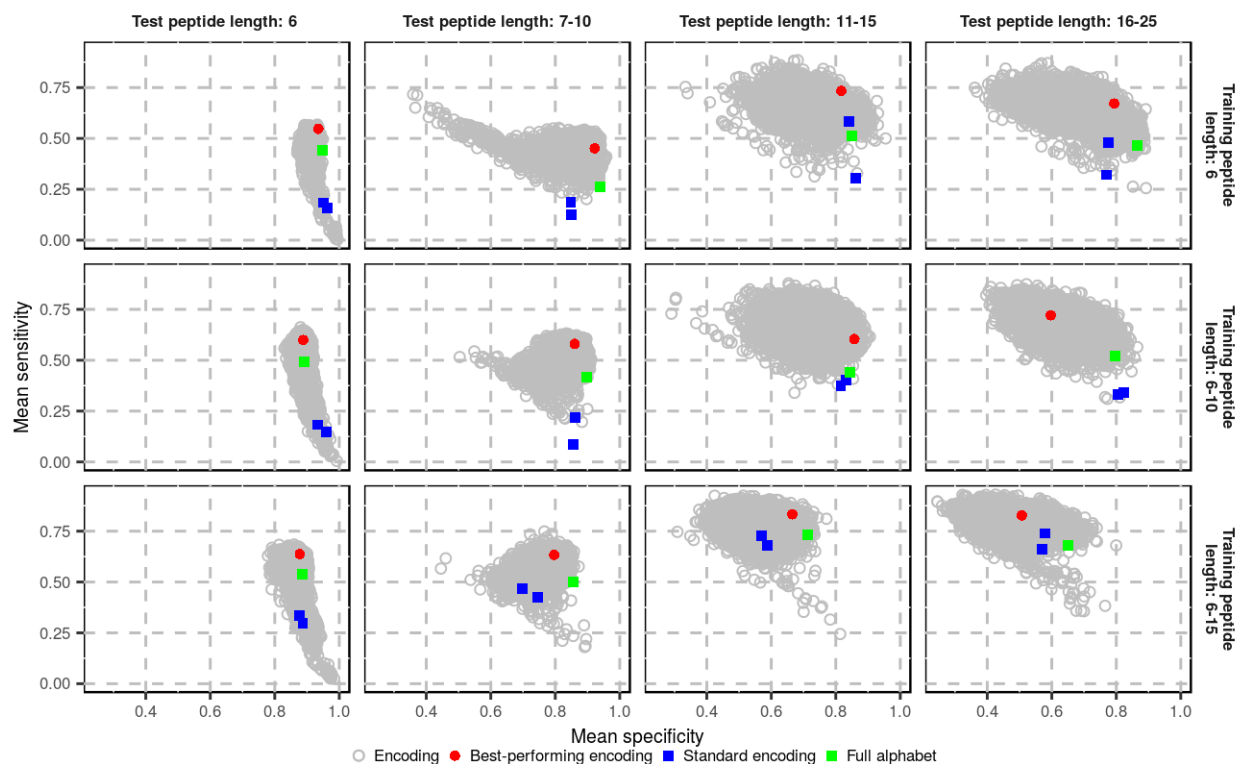


**Figure 3.** Sensitivity and specificity of classifiers with various encodings for every possible combination of sequence lengths in the training and testing data sets. The classifier based on the best-performing encoding always have good specificity and sensitivity.



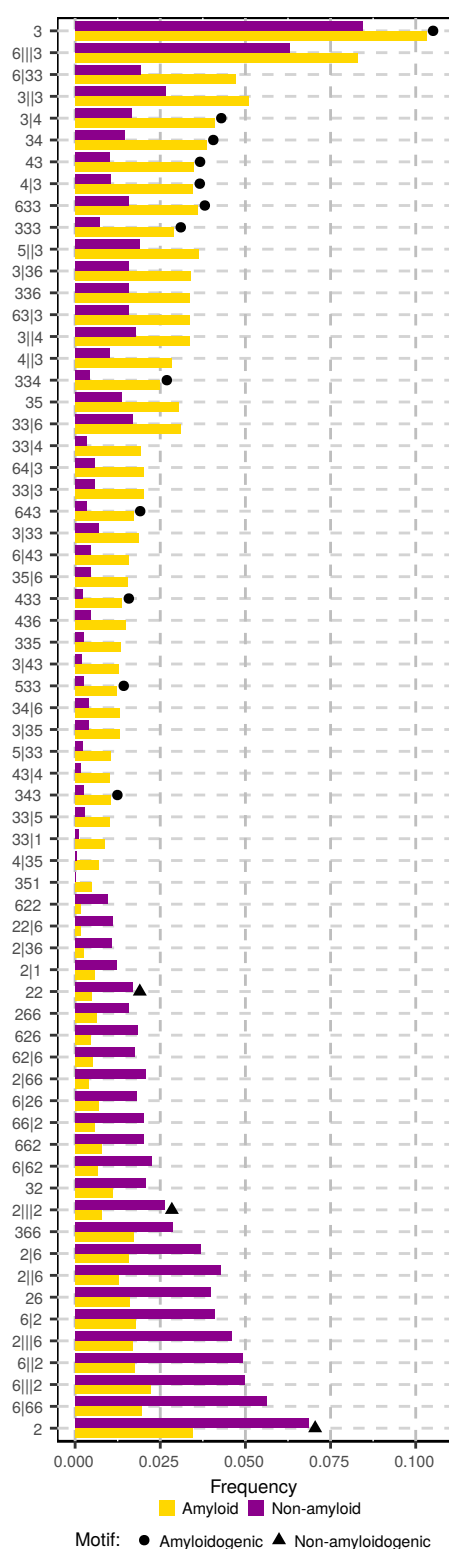


**Figure 5.** The frequency of important n-grams used by the best-performing classifier in amyloid and non-amyloid sequences. The elements of n-grams are amino acids encoded using the best-performing reduced amino acid alphabet (see Tab. 3). A vertical bar represents a gap in a n-gram between its elements. The frequency was computed using the total number of occurrences divided by the number of possible n-grams of this length. Dots and triangles denote n-grams occurring in motifs found in respectively amyloidogenic and non-amyloidogenic sequences (?).

**Table 3.** The best-performing encoding.

Subgroup ID	Amino acids
1	G
2	K, P, R
3	I, L, V
4	F, W, Y
5	A, C, H, M
6	D, E, N, Q, S, T

The best encoding chosen in the analysis consists of six amino acid subgroups, which are characterized by distinct and specific properties (Tab. 3). The 3rd subgroup contains strongly hydrophobic amino acids. In the 4th subgroup, the amino acids show also aromatic properties. On the other hand, the most hydrophilic amino acids are in the 2nd and 6th subgroups. The former includes two clear basic amino acids, whereas the latter two acidic and four polar residues. The first subgroup includes only glycine, which is the smallest amino acid and the most flexible. By average, quite flexible amino acids are also present in the 2nd subgroup, whereas the least flexible amino acids are in the subgroup 4 and 5. The glycine has also the lowest propensity to form  $\beta$ -sheet and the subgroups 3 and 4 largest.

To compare the best-performing encoding to other encodings, we calculated encoding distances between them (Fig. 4). To compute the scale factor, we used normalized values of described above four features. The value of AUC is significantly lower for more distant encodings ( $-0.437$  Pearson's correlation coefficient, p-value smaller than  $2.2 \times 10^{-16}$ ). Such relationship indicates that the best-performing encoding was not found by chance and inclusion of properties reflected by this encoding improves the prediction of amyloids.

We selected 65 n-grams that obtained p-values smaller than 0.05 in QuiPT test in all repetitions of cross-validation regardless of the length of sequences in the training set (see Fig. 5). The frequency of the n-grams was computed for all sequences derived from AmyLoad database. The n-grams typical of amyloidogenic sequences (with the highest frequency in amyloids) incorporate mostly highly hydrophobic amino acids with tendency to form  $\beta$ -structures, from subgroups 3 and 4. The n-grams occurring frequently in amyloids have often repeats of amino acids from the subgroup 3, suggesting that the presence of these amino acids in vicinity might be one of the most effective predictors of amyloidogenicity.

On the other hand, n-grams typical of non-amyloidogenic peptides have mostly amino acids belonging to subgroups 2 and 6 which include strongly hydrophilic and highly flexible amino acids, which may hamper forming  $\beta$ -structures.

### Benchmark of AmyloGram

The benchmark covered AmyloGram as well as three peer-reviewed predictors of amyloidogenicity: PASTA2 (33), FoldAmyloid (2) and APPNN (34). Other classifiers published before were not included in the benchmark because their performance on *pep424* data set is already known and lower than the performance of PASTA2 and FoldAmyloid (33).

**Table 4.** Results of benchmark on *pep424* data set for PASTA2, FoldAmyloid, AmyloGram and random forest predictor learned on n-grams extracted for full amino acid alphabet from the sequences with the length specified in the brackets (FA).

Classifier	AUC	MCC	Sensitivity	Specificity
AmyloGram	<b>0.8972</b>	<b>0.6307</b>	0.8658	0.7889
full alphabet (6)	0.8411	0.5427	0.4966	<b>0.9593</b>
full alphabet (6-10)	0.8581	0.5698	0.7517	0.8259
full alphabet (6-15)	0.8610	0.5490	0.8188	0.7519
PASTA2	0.8550	0.4291	0.3826	0.9519
FoldAmyloid	0.7351	0.4526	0.7517	0.7185
APPNN	0.8343	0.5823	<b>0.8859</b>	0.7222

We analyzed Area Under the Curve (AUC), Matthew's Correlation Coefficient (MCC), sensitivity and specificity (see Tab. 4). We used default settings for FoldAmyloid and PASTA2 evaluated input data in the 'Peptides' mode.

Since PASTA2 does not return a probability of belonging to specific category, we normalized the output data to compute the AUC values. The advised energy threshold (-5) was also normalized in the same manner and used as cut-off in computations of specificity, sensitivity and MCC. The resulting value of specificity 0.9519 is close to the value provided by authors (0.95) and assures correctness of our computations. For other classifiers, we assumed 0.5 cut-off.

In the case of the studied data set, the n-gram extraction method appeared efficient enough to produce classifiers able to outperformed the published methods. AmyloGram showed the highest AUC and MCC among all tested classifiers. It had lower specificity than two n-gram classifiers trained on the full alphabet but still outperformed two other published method in this category. It is important to highlight that AmyloGram is the most balanced among all analyzed classifiers, having the best specificity/sensitivity trade-off, as indicated by the value of MCC.

The specificity of AmyloGram is lower than the specificity of PASTA2 but it is a consequence of the usage of the threshold value optimized for 0.95 specificity for the latter. If we assume for the AmyloGram the same threshold for the specificity, our classifier will have still higher sensitivity (0.5518) than PASTA2. Therefore, if we assume thresholds to both predictors detect true non-amyloids with the same accurateness, AmyloGram predicts more true amyloids.

Two of three classifiers based on n-gram and trained on the full alphabet had also AUC higher than PASTA2 and all three were more successful than FoldAmyloid as well as APPNN. They also maintained the high specificity as seen previously during cross-validation. However, they generally performed worse than the classifier based on reduced amino acid alphabet.

Among all considered predictors of amyloidogenicity, APPNN had the highest sensitivity. Nevertheless, its AUC was worse than AUCs of all n-gram-based predictors as well as PASTA2 indicating lower overall performance.

AmyloGram is trained to predict amyloidogenic, not amyloidic regions. Hence, we did not tested it on *reg33* data set, which is commonly used to detect the performance

in prediction of all regions participating in the amyloid aggregation (?).

### AmyloGram web server

Our software is accessible as the web server under address [www.smorfland.uni.wroc.pl/amylogram/](http://www.smorfland.uni.wroc.pl/amylogram/). AmyloGram is also accessible in the batch mode as the R package (ADDRESS).

### CONCLUSION

Thanks to the reduction of amino acid alphabet, we were able to create the efficient predictor of amyloidogenic sequences called AmyloGram. One of the strength of our approach is its highly interpretable outcome, which hopefully sheds new light on the process of amyloid aggregation.

The idea of using the encodings is a proven concept. We employed it in our innovative framework to generate and validate several thousands of possible amino acid encodings. Due to this approach, we were able to specify important physicochemical properties that define the best-performing alphabet and thereby extract features associated with amyloidogenicity, such as hydrophobicity and tendency to forming  $\beta$ -sheets. In addition to them, we discovered a new property, i.e. flexibility.

Our analysis was completed with the extraction of important n-grams, which might be interpreted as short motifs highly relevant to amyloidogenicity or non-amyloidogenicity of peptides. Sixty five important n-grams revealed that mostly alifatic and nonpolar amino acids (isoleucine, leucine and valine) together with aromatic and also hydrophobic amino acids (phenylalanine, tyrosine, tryptophan) are good predictors of amyloids.

Since the best-performing classifier was trained on the alphabet consisting of six amino acid groups, it still outperformed predictors learning on the raw amino acid sequences and is enough to find n-grams separating efficiently amyloids and non-amyloids.

### FUNDING

Computations were carried out in Wroclaw Center for Networking and Supercomputing (<http://www.wcss.pl>) and funded by the institutional grant No. 347.

This research was funded by the KNOW Consortium and National Science Center (2015/17/N/NZ2/01845).

### REFERENCES

1. Härd, T. and Lendel, C. (August, 2012) Inhibition of Amyloid Formation. *Journal of Molecular Biology*, **421**(4–5), 441–465.
2. Garbuzynskiy, S. O., Lobanov, M. Y., and Galzitskaya, O. V. (February, 2010) FoldAmyloid: a method of prediction of amyloidogenic regions from protein sequence. *Bioinformatics (Oxford, England)*, **26**(3), 326–332.
3. Bryan, A. W., O'Donnell, C. W., Menke, M., Cowen, L. J., Lindquist, S., and Berger, B. (February, 2012) STITCHER: Dynamic assembly of likely amyloid and prion -structures from secondary structure predictions. *Proteins*, **80**(2), 410–420.
4. Goldschmidt, L., Teng, P. K., Riek, R., and Eisenberg, D. (February, 2010) Identifying the amyloids, proteins capable of forming amyloid-like fibrils. *Proceedings of the National Academy of Sciences*, **107**(8), 3487–3492.
5. O'Donnell, C. W., Waldisphl, J., Lis, M., Halfmann, R., Devadas, S., Lindquist, S., and Berger, B. (July, 2011) A method for probing the



- mutational landscape of amyloid structure. *Bioinformatics*, **27**(13), i34–i42.
6. Beerten, J., Van Durme, J., Gallardo, R., Capriotti, E., Serpell, L., Rousseau, F., and Schymkowitz, J. (May, 2015) WALTZ-DB: a benchmark database of amyloidogenic hexapeptides. *Bioinformatics (Oxford, England)*, **31**(10), 1698–1700.
  7. Gasior, P. and Kotulska, M. (February, 2014) FISH Amyloid a new method for finding amyloidogenic segments in proteins based on site specific co-occurrence of aminoacids. *BMC Bioinformatics*, **15**(1), 54.
  8. Stanislawski, J., Kotulska, M., and Unold, O. (2013) Machine learning methods can replace 3D profile method in classification of amyloidogenic hexapeptides. *BMC Bioinformatics*, **14**, 21.
  9. Zambrano, R., Jamroz, M., Szczasiuk, A., Pujols, J., Kmiecik, S., and Ventura, S. (April, 2015) AGGRESKAN3D (A3D): server for prediction of aggregation properties of protein structures. *Nucleic Acids Research*, p. gkv359.
  10. Murphy, L. R., Wallqvist, A., and Levy, R. M. (March, 2000) Simplified amino acid alphabets for protein fold recognition and implications for folding. *Protein Engineering*, **13**(3), 149–152.
  11. Breiman, L. (October, 2001) Random Forests. *Machine Learning*, **45**(1), 5–32.
  12. Wozniak, P. P. and Kotulska, M. (June, 2015) AmyLoad: website dedicated to amyloidogenic protein fragments. *Bioinformatics (Oxford, England)*,.
  13. Kawashima, S., Pokarowski, P., Pokarowska, M., Kolinski, A., Katayama, T., and Kanehisa, M. (January, 2008) AAindex: amino acid index database, progress report 2008. *Nucleic Acids Research*, **36**(suppl 1), D202–D205.
  14. Wozniak, P. P. and Kotulska, M. (2014) Characteristics of protein residue-residue contacts and their application in contact prediction. *Journal of Molecular Modeling*, **20**(11).
  15. Joe H. Ward Jr (March, 1963) Hierarchical Grouping to Optimize an Objective Function. *Journal of the American Statistical Association*, **58**(301), 236–244.
  16. Bhaskaran, R. and Ponnuswamy, P. (October, 1988) Positional flexibilities of amino acid residues in globular proteins. *International Journal of Peptide and Protein Research*, **32**(4), 241–255.
  17. Nishikawa, K. and Ooi, T. (October, 1986) Radial locations of amino acid residues in a globular protein: correlation with the sequence. *Journal of Biochemistry*, **100**(4), 1043–1047.
  18. Radzicka, A. and Wolfenden, R. (March, 1988) Comparing the polarities of the amino acids: side-chain distribution coefficients between the vapor phase, cyclohexane, 1-octanol, and neutral aqueous solution. *Biochemistry*, **27**(5), 1664–1670.
  19. Zhou, H. and Zhou, Y. (February, 2004) Quantifying the effect of burial of amino acid residues on protein stability. *Proteins*, **54**(2), 315–322.
  20. Kanehisa, M. I. and Tsong, T. Y. (September, 1980) Local hydrophobicity stabilizes secondary structures in proteins. *Biopolymers*, **19**(9), 1617–1628.
  21. Prabhakaran, M. (August, 1990) The distribution of physical, chemical and conformational properties in signal and nascent peptides. *The Biochemical Journal*, **269**(3), 691–696.
  22. Kim, C. A. and Berg, J. M. (March, 1993) Thermodynamic beta-sheet propensities measured using a zinc-finger host peptide. *Nature*, **362**(6417), 267–270.
  23. Argos, P., Rao, J. K., and Hargrave, P. A. (November, 1982) Structural prediction of membrane-bound proteins. *European journal of biochemistry / FEBS*, **128**(2-3), 565–575.
  24. Sweet, R. M. and Eisenberg, D. (December, 1983) Correlation of sequence hydrophobicities measures similarity in three-dimensional protein structure. *Journal of Molecular Biology*, **171**(4), 479–488.
  25. Kidera, A., Konishi, Y., Oka, M., Ooi, T., and Scheraga, H. A. (February, 1985) Statistical analysis of the physical properties of the 20 naturally occurring amino acids. *Journal of Protein Chemistry*, **4**(1), 23–55.
  26. Black, S. D. and Mould, D. R. (February, 1991) Development of hydrophobicity parameters to analyze proteins which bear post- or cotranslational modifications. *Analytical Biochemistry*, **193**(1), 72–82.
  27. Charton, M. and Charton, B. I. (December, 1982) The structural dependence of amino acid hydrophobicity parameters. *Journal of Theoretical Biology*, **99**(4), 629–644.
  28. Pontius, J., Richelle, J., and Wodak, S. J. (November, 1996) Deviations from Standard Atomic Volumes as a Quality Measure for Protein Crystal Structures. *Journal of Molecular Biology*, **264**(1), 121–136.
  29. Takano, K. and Yutani, K. (August, 2001) A new scale for side-chain contribution to protein stability based on the empirical stability analysis of mutant proteins. *Protein Engineering*, **14**(8), 525–528.
  30. Kotulska, M. and Unold, O. (December, 2013) On the amyloid datasets used for training PAFIG: how (not) to extend the experimental dataset of hexapeptides. *BMC Bioinformatics*, **14**, 351.
  31. Lehmann, E. L. and Romano, J. P. (August, 2008) Testing Statistical Hypotheses, Springer New York, .
  32. Wright, M. N. and Ziegler, A. (August, 2015) ranger: A Fast Implementation of Random Forests for High Dimensional Data in C++ and R. *arXiv:1508.04409 [stat]*, arXiv: 1508.04409.
  33. Walsh, I., Seno, F., Tosatto, S. C. E., and Trovato, A. (May, 2014) PASTA 2.0: an improved server for protein aggregation prediction. *Nucleic Acids Research*, p. gku399.
  34. Famlia, C., Dennison, S. R., Quintas, A., and Phoenix, D. A. (August, 2015) Prediction of Peptide and Protein Propensity for Amyloid Formation. *PLOS ONE*, **10**(8), e0134679.